Dynamic Functional Relay between Insulin Receptor Substrate 1 and 2 in Hepatic Insulin Signaling during Fasting and Feeding

Naoto Kubota,[1,2,3,13] Tetsuya Kubota,[1,3,4,13] Shinsuke Itoh,[1,5,13] Hiroki Kumagai,[1] Hideki Kozono,[1] Iseki Takamoto,[1,3]
Tomoka Mineyama,[1] Hitomi Ogata,[6] Kumpei Tokuyama,[6] Mitsuru Ohsugi,[1] Takayoshi Sasako,[1] Masao Moroi,[4]
Kaoru Sugi,[4] Shigeru Kakuta,[7] Yoichiro Iwakura,[7] Tetsuo Noda,[8] Shin Ohnishi,[9] Ryozo Nagai,[2,10] Kazuyuki Tobe,[11]
Yasuo Terauchi,[12] Kohjiro Ueki,[1,2] and Takashi Kadowaki[1,2,*]
[1]Department of Diabetes and Metabolic Diseases, Graduate School of Medicine
[2]Translational Systems Biology and Medicine Initiative (TSBMI)
University of Tokyo, Tokyo, Japan
[3]Clinical Nutrition Program, National Institute of Health and Nutrition, Tokyo, Japan
[4]Division of Cardiovascular Medicine, Toho University, Ohashi Hospital, Tokyo, Japan
[5]Kowa Company Limited, Tokyo, Japan
[6]Graduate School of Comprehensive Human Sciences, University of Tsukuba, Tsukuba, Japan
[7]Center for Experimental Medicine, Institute of Medical Science, University of Tokyo, Tokyo, Japan
[8]Department of Cell Biology, Japanese Foundation for Cancer Research, Cancer Institute, Tokyo, Japan
[9]Department of Gastroenterology, Graduate School of Medicine
[10]Department of Cardiovascular Diseases, Graduate School of Medicine
University of Tokyo, Tokyo, Japan
[11]First Department of Internal Medicine, Faculty of Medicine, University of Toyama, Toyama, Japan
[12]Department of Diabetes and Endocrinology, Yokohama City University, School of Medicine, Kanagawa, Japan
[13]These authors contributed equally to this work.
*Correspondence: kadowaki-3im@h.u-tokyo.ac.jp
DOI 10.1016/j.cmet.2008.05.007

SUMMARY

Insulin receptor substrate (Irs) mediates metabolic actions of insulin. Here, we show that hepatic Irs1 and Irs2 function in a distinct manner in the regulation of glucose homeostasis. The PI3K activity associated with Irs2 began to increase during fasting, reached its peak immediately after refeeding, and decreased rapidly thereafter. By contrast, the PI3K activity associated with Irs1 began to increase a few hours after refeeding and reached its peak thereafter. The data indicate that Irs2 mainly functions during fasting and immediately after refeeding, and Irs1 functions primarily after refeeding. In fact, liver-specific Irs1-knockout mice failed to exhibit insulin resistance during fasting, but showed insulin resistance after refeeding; conversely, liver-specific Irs2-knockout mice displayed insulin resistance during fasting but not after refeeding. We propose the concept of the existence of a dynamic relay between Irs1 and Irs2 in hepatic insulin signaling during fasting and feeding.
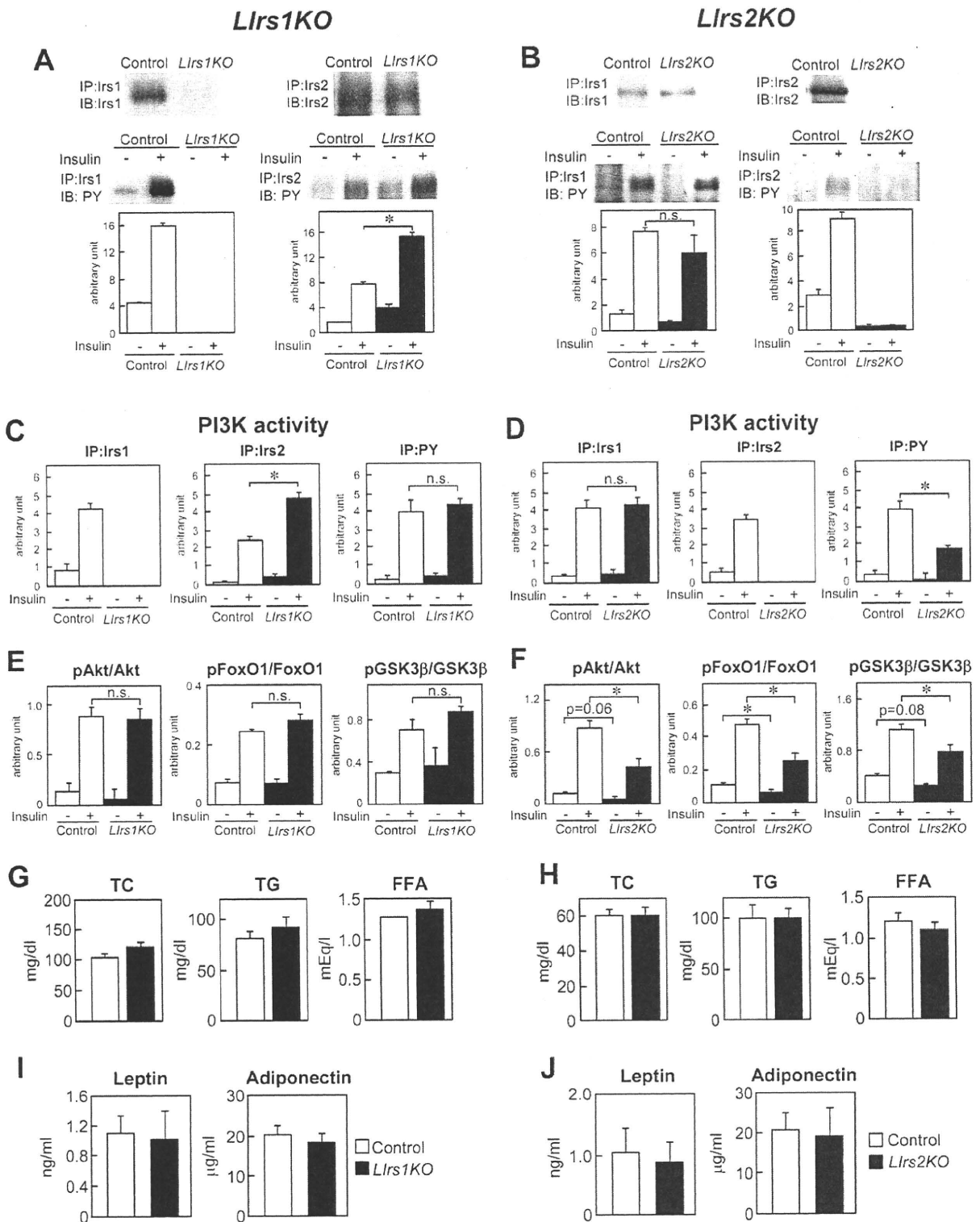
INTRODUCTION

The liver is an essential organ for glucose homeostasis; it stores excess glucose after food intake in the form of glycogen and releases glucose by glycogenolysis or gluconeogenesis during fasting (Gribble, 2005). Insulin promotes glycogen synthesis and inhibits glycogenolysis and gluconeogenesis by exerting direct and indirect effects on the enzyme activities and gene expressions in the liver (Saltiel and Kahn, 2001). Dysregulation of the hepatic insulin actions is a critical component in the pathogenesis of type 2 diabetes (Saltiel and Kahn, 2001).

Recently, it was reported that circulating insulin not only directly inhibits glucose production in the liver, but also acts at the level of the brain to suppress gluconeogenesis (Wada et al., 2005; Kasuga, 2006; Plum et al., 2006). Downregulation of the hypothalamic insulin receptor caused hepatic insulin resistance (Obici et al., 2002a), and intracerebroventricular injection of insulin suppressed hepatic glucose production (Obici et al., 2002b), suggesting that insulin inhibits hepatic glucose production via both the classical direct hepatic pathway and a newly identified central indirect pathway. Considering this indirect central action of insulin, it was considered that genetically engineered animals lacking in insulin signaling exclusively in the liver may be useful models for clarifying the physiological roles of the direct effects of insulin in the liver. In fact, mice with genetic deletion of the hepatic insulin receptors (*LIRKO* mice) were found to exhibit severe insulin resistance and hyperglycemia after feeding, indicating that hepatic insulin-receptor signaling plays a pivotal role in the regulation of hepatic and systemic glucose homeostasis (Michael et al., 2000).

Insulin receptor substrate (Irs) 1 and Irs2 exhibit high structural homology, are abundantly expressed in the liver, and are thought to be responsible for transmitting insulin signaling from the insulin receptor to the intracellular effectors in the regulation of glucose and lipid homeostasis (Saltiel and Kahn, 2001; Nandi et al., 2004; Taniguchi et al., 2006; Thirone et al., 2006). However, while mice lacking in systemic Irs1 failed to show any impairment

LIrs1KO

LIrs2KO

of hepatic insulin signaling (Tamemoto et al., 1994; Araki et al., 1994; Tobe et al., 1995; Yamauchi et al., 1996), those lacking in systemic Irs2 exhibited impaired hepatic insulin signaling and impaired suppression of glucose production by insulin (Withers et al., 1998; Kubota et al., 2000). Hyperinsulinemic-euglycemic clamp studies have revealed that systemic Irs2-knockout mice show markedly impaired suppression of hepatic glucose production and reduced stimulation of liver glycogen synthesis, while systemic Irs1-knockout mice show insulin resistance predominantly in the skeletal muscle and adipose tissue but not in the liver (Previs et al., 2000). These data point to the significance of liver Irs2 and/or brain Irs2 in the hepatic actions of insulin.

Recently, liver-specific Irs2-knockout mice were generated, which unexpectedly exhibited little or no disturbance of glucose homeostasis (Dong et al., 2006; Simmgen et al., 2006). Considering the severe insulin resistance and hyperglycemia observed after feeding in the LIRKO mice (Michael et al., 2000), these data led us to re-examine the role of Irs1, the other major Irs protein in the liver. In this study, we generated liver-specific Irs1-knockout mice, as well as liver-specific Irs2-knockout mice, to investigate the physiological roles of hepatic Irs1 and Irs2 in the regulation of glucose metabolism. Furthermore, we also generated liver-specific Irs1/Irs2 double-knockout mice in an attempt to elucidate whether hepatic insulin signaling is exclusively mediated by Irs1 and Irs2.

RESULTS

Generation of Liver-Specific Irs1- and Irs2-Knockout Mice

Genomic DNA PCR was performed to detect Cre-mediated recombination at the genomic DNA level. The *Irs1* and *Irs2* alleles were found to be deleted in the livers of the liver-specific Irs1-knockout (*LIrs1KO*) and liver-specific Irs2-knockout (*LIrs2KO*) mice, respectively, but not in any of the tissues in the control mice (Figure S1A). While the *Irs1* mRNA was almost completely abrogated, the *Irs2* mRNA levels remained unchanged in the *LIrs1KO* mice; conversely, while the *Irs1* mRNA levels remained unchanged, the *Irs2* mRNA was almost completely abrogated in the *LIrs2KO* mice (Figure S1B). Western blotting of the Irs1 or Irs2 immunoprecipitates from the livers of the control and *LIrs1KO* mice under the fasting condition revealed that while expression of the Irs1 protein was almost completely abrogated in the *LIrs1KO* mice, the expression level of the Irs2 protein was indistinguishable from that in the control mice (Figure 1A, upper panels). When insulin was administered via the inferior vena

cava under the fasting condition, tyrosine phosphorylation of Irs1 (Figure 1A, lower-left panels) and insulin-stimulated recruitment of the p85-adaptor subunit of phosphatidylinositol 3-kinase (PI3K) to the Irs1 immunoprecipitates (Figure S2A, left panels) were also abrogated in the *LIrs1KO* mice. On the other hand, insulin-stimulated tyrosine phosphorylation of Irs2 (Figure 1A, lower-right panels) and insulin-stimulated recruitment of the p85-adaptor subunit of PI3K to the Irs2 immunoprecipitates (Figure S2A, right panels) were significantly increased in these *LIrs1KO* mice, similar to the findings in systemic, Irs1-deficient mice (Tobe et al., 1995; Yamauchi et al., 1996). On the other hand, in the *LIrs2KO* mice, the Irs2 protein was almost completely abrogated, while the expression level of the Irs1 protein was indistinguishable from that in the control mice (Figure 1B, upper panels). While insulin-stimulated tyrosine phosphorylation of Irs2 (Figure 1B, lower-right panels) and insulin-stimulated recruitment of the p85-adaptor subunit of PI3K to the Irs2 immunoprecipitates (Figure S2B, right panels) were abrogated in these *LIrs2KO* mice, insulin-stimulated tyrosine phosphorylation of Irs1 (Figure 1B, lower-left panels) and insulin-stimulated recruitment of the p85-adaptor subunit of PI3K to Irs1 immunoprecipitates (Figure S2B, left panels) under the fasting condition were similar between the control and *LIrs2KO* mice, similar to the findings in systemic, Irs2-deficient mice (Kubota et al., 2000). When lysates from the livers of fasted *LIrs1KO* mice were immunoprecipitated with anti-Irs1 antibody, the insulin-stimulated PI3K activity associated with Irs1 was completely abrogated (Figures 1C, left panel, and S2C, left panel), while that associated with Irs2 was ~2-fold as high as that in the control mice (Figures 1C, middle panel, and S2C, middle panel). Thus, insulin-stimulated PI3K activity associated with tyrosine-phosphorylated proteins was similar between the two genotypes under the fasting condition (Figures 1C, right panel, and S2C, right panel). On the other hand, in fasted *LIrs2KO* mice, insulin-stimulated PI3K activity associated with Irs2 was completely abrogated (Figures 1D, middle panel, and S2D, middle panel), while that associated with Irs1 was similar to that in the control mice (Figures 1D, left panel, and S2D, left panel). Consequently, insulin-stimulated PI3K activity associated with tyrosine-phosphorylated proteins was reduced by half in the *LIrs2KO* mice as compared with that in the control mice (Figures 1D, right panel, and S2D, right panel). Basal and insulin-stimulated phosphorylation of Akt, forkhead transcription factor O1 (FoxO1), and glycogen synthase kinase (GSK)3β, which are all among the major substrates of Akt, were similar in the liver of the control and *LIrs1KO* mice under the fasting condition (Figures 1E and S2E). In contrast, basal phosphorylation of Akt and GSK3β tended to be

---

Figure 1. Generation of the LIrs1KO and LIrs2KO Mice
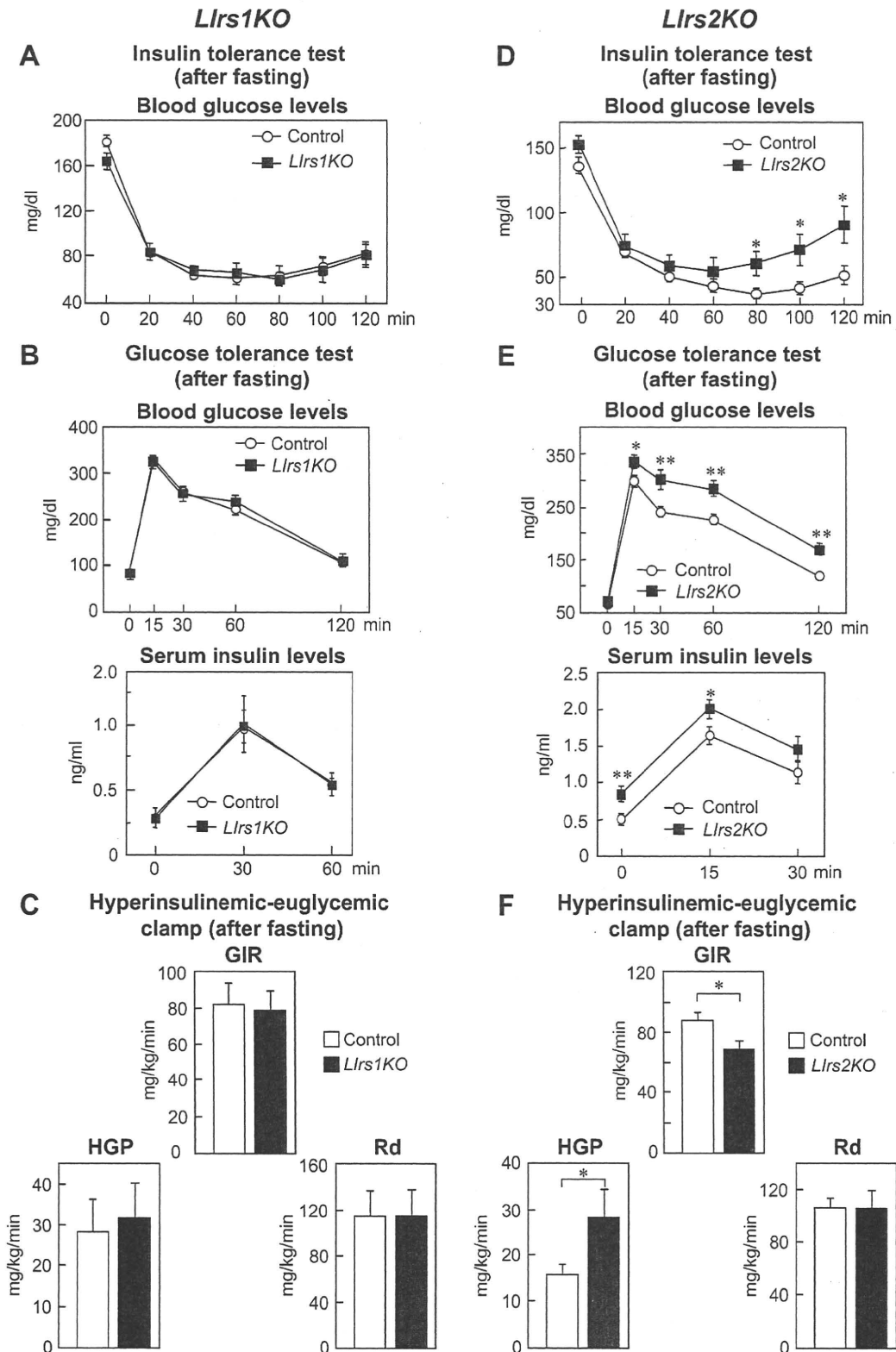
(A and B) Upper panels show liver lysates from *LIrs1KO* (A) and *LIrs2KO* (B) mice were immunoprecipitated with anti-Irs1 or anti-Irs2 antibody and subsequently immunoblotted with anti-Irs1 or anti-Irs2 antibody after overnight (about 16 hr) fasting. Lower panels show insulin-stimulated tyrosine phosphorylation of Irs1 or Irs2 at 70 s after administration of 10 U of insulin in the liver of the *LIrs1KO* (A) and *LIrs2KO* (B) mice after overnight (about 16 hr) fasting. Results are representative of three independent experiments.

(C and D) Insulin-stimulated PI3K activity associated with Irs1-, Irs2-, and tyrosine-phosphorylated proteins at 70 s after administration of 10 U of insulin in the liver of the *LIrs1KO* (C) and *LIrs2KO* (D) mice after overnight (about 16 hr) fasting. Results are representative of three independent experiments.

(E and F) Insulin-stimulated phosphorylation of Akt, FoxO1, and GSK3β at 70 s after administration of 10 U of insulin in the liver of the *LIrs1KO* (E) and *LIrs2KO* (F) mice after overnight (about 16 hr) fasting. Results are representative of three independent experiments.

(G and H) Serum levels of TC, TG, and FFA in 8-week-old *LIrs1KO* (G) and *LIrs2KO* (H) mice after overnight (about 16 hr) fasting (n = 11–17).

(I and J) Serum leptin and adiponectin levels in 8-week-old *LIrs1KO* (I) and *LIrs2KO* (J) mice after overnight (about 16 hr) fasting (n = 6–11). All the experiments illustrated in this figure were performed using 8- to 10-week-old male mice, unless otherwise specified. Results are represented as mean ± SEM *p < 0.05.

LIrs1KO

A
Insulin tolerance test
(after fasting)
Blood glucose levels

B
Glucose tolerance test
(after fasting)
Blood glucose levels

Serum insulin levels

C
Hyperinsulinemic-euglycemic
clamp (after fasting)
GIR

HGP

Rd

LIrs2KO

D
Insulin tolerance test
(after fasting)
Blood glucose levels

E
Glucose tolerance test
(after fasting)
Blood glucose levels

Serum insulin levels

F
Hyperinsulinemic-euglycemic
clamp (after fasting)
GIR

HGP

Rd

reduced, and that of FoxO1 was significantly reduced in the livers of the *LIrs2KO* mice (Figures 1F and S2F). Insulin-stimulated phosphorylation of Akt, FoxO1, and GSK3β was also significantly reduced in the livers of the *LIrs2KO* mice (Figures 1F and S2F). We next measured insulin-stimulated phosphorylation of Irs1, Irs2, Akt, and FoxO1 at 30 min after administration of 0.1 U of insulin in the livers of the *LIrs1KO* and *LIrs2KO* mice to investigate the events as they might occur under more physiological conditions. The insulin-stimulated phosphorylation levels of Irs1, Irs2, Akt, and FoxO1 remained essentially the same in the *LIrs1KO* (Figure S2G) and *LIrs2KO* (Figure S2H) mice, regardless of the dose of insulin. These data indicate that the potentially reduced insulin-stimulated PI3K activity following acute or subacute administration of insulin under the fasting condition is compensated for in the *LIrsKO* mice by increased tyrosine phosphorylation of Irs2, whereas that in the *LIrs2KO* mice is not compensated for by increased tyrosine phosphorylation of Irs1. The serum levels of total cholesterol (TC), triglyceride (TG), and free fatty acid (FFA) were similar between the control and *LIrsKO* mice (Figure 1G) or between the control and *LIrs2KO* mice (Figure 1H) under the fasting condition. In addition, the serum leptin and adiponectin levels were also not significantly different between the control and *LIrsKO* mice (Figure 1I) or between the control and *LIrs2KO* mice (Figure 1J), under the fasting condition.

LIrs2KO (but Not *LIrs1KO*) Mice Showed Insulin Resistance under the Fasting Condition

LIrsKO mice showed similar body-weight gain to the control mice (data not shown), unlike the finding reported previously in systemic Irs1-deficient mice (Tamemoto et al., 1994; Araki et al., 1994). An insulin-tolerance test (ITT) conducted after fasting revealed that the glucose-lowering effect of insulin was similar between the control and *LIrs1KO* mice (Figure 2A). In the oral-glucose-tolerance test (OGTT) conducted after fasting, the blood glucose and serum insulin levels before and after glucose loading were not significantly different between the two mouse genotypes (Figure 2B). We next carried out a hyperinsulinemic-euglycemic clamp study in the animals under the fasting condition. None of the parameters (i.e., the glucose infusion rate [GIR]), hepatic glucose production (HGP), or the rate of glucose disappearance (R_d) differed significantly between the control and *LIrs1KO* mice (Figure 2C), indicating that *LIrs1KO* mice do not exhibit insulin resistance or glucose intolerance under the fasting condition.

LIrs2KO mice also showed similar body-weight gain to the control mice, unlike the finding reported previously in the systemic Irs2-deficient mice (Tobe et al., 2001). An ITT conducted after fasting revealed insulin resistance in the *LIrs2KO* mice (Figure 2D). In the OGTT conducted after fasting, the blood glucose levels after glucose loading (Figure 2E, upper

panel), as well as the serum insulin levels (Figure 2E, lower panel) before and after glucose loading, were significantly elevated in these mice. In the hyperinsulinemic-euglycemic clamp study conducted under the fasting condition, the GIR was significantly lower and the HGP significantly higher in the *LIrs2KO* mice than in the control mice, whereas no significant difference in the R_d was noted between the two mouse genotypes (Figure 2F). These findings indicate that the *LIrs2KO* mice show hepatic insulin resistance under the fasting condition. In the skeletal muscle (Figures S3A and S3B) and white adipose tissue (Figures S3C and S3D), basal- and insulin-stimulated phosphorylation of Akt was similar between the control and *LIrs1KO* mice or between the control and *LIrs2KO* mice, indicating that insulin signaling was not impaired in either the skeletal muscle or white adipose tissue of the *LIrs1KO* and *LIrs2KO* mice under the fasting condition. There were no significant histological changes in the livers of either the *LIrs1KO* or *LIrs2KO* mice (Figure S4A), unlike the observations in the *LIRsKO* mice (Michael et al., 2000). The fasting TG content in the liver (Figure S4B), the serum aspartate aminotransferase (AST), and alanine aminotransferase (ALT) (Figure S4C) levels also showed no significant differences in the *LIrs1KO* and *LIrs2KO* mice as compared with the findings in the control mice, suggesting that disruption of Irs1 or Irs2 does not cause any significant hepatic disorder.

LIrs1KO (but Not *LIrs2KO*) Mice Exhibited Insulin Resistance under the Refeeding Condition

Since insulin regulates glucose homeostasis in the liver not only during fasting but also after refeeding, the insulin sensitivity and insulin signaling under the refeeding condition were also examined in the knockout mice. Unexpectedly, the ITT revealed insulin resistance in the *LIrs1KO* mice at 6 hr after the start of refeeding following 24 hr of fasting (Figure 3A), unlike under the fasting condition (Figure 2A). The GIR was significantly lower (and the HGP significantly higher) in the *LIrs1KO* mice as compared with the values in the control mice under the refeeding condition (Figure 3B), unlike under the fasting condition (Figure 2C). In contrast to these findings in the *LIrs1KO* mice, the ITT revealed insulin resistance under the fasting condition (Figure 2D) but not under the refeeding condition (Figure 3C) in the *LIrs2KO* mice. Unlike the observations under the fasting condition in these animals (Figure 2F), no significant differences in the GIR, HGP, or R_d were found between the control and *LIrs2KO* mice under the refeeding condition (Figure 3D). Significantly reduced phosphorylation of Akt, FoxO1, and GSK3β was observed after refeeding, but not under the fasting condition, in the livers of the *LIrs1KO* mice (Figures 3E and S5A). The hepatic glycogen content was also decreased significantly in these mice after refeeding, but not under the fasting condition (Figure 3F). While the expression levels of PEPCK and G6Pase showed no significant differences

---

Figure 2. *LIrs2KO* (but Not *LIrs1KO*) Mice Showed Insulin Resistance and Glucose Intolerance under the Fasting Condition

(A) ITT in 8-week-old control and *LIrs1KO* mice after 3 hr fasting (n = 25–27).

(B) Blood glucose and serum insulin levels in 8-week-old control and *LIrs1KO* mice during an OGTT conducted after 24 hr fasting (n = 22).

(C) GIR, HGP, and R_d in control and *LIrs1KO* mice in the hyperinsulinemic-euglycemic clamp study conducted after 6 hr fasting (n = 5).

(D) ITT in 8-week-old control and *LIrs2KO* mice after 3 hr fasting (n = 17–19).

(E) Blood glucose and serum insulin levels in 8-week-old control and *LIrs2KO* mice during an OGTT conducted after 24 hr fasting (n = 17–19).

(F) GIR, HGP, and R_d in control and *LIrs2KO* mice in the hyperinsulinemic-euglycemic clamp study conducted after 6 hr fasting (n = 6–10). All the experiments illustrated in this figure were performed using 8- to 10-week-old male mice, unless otherwise specified. Results are represented as mean ± SEM *p < 0.05, **p < 0.01.
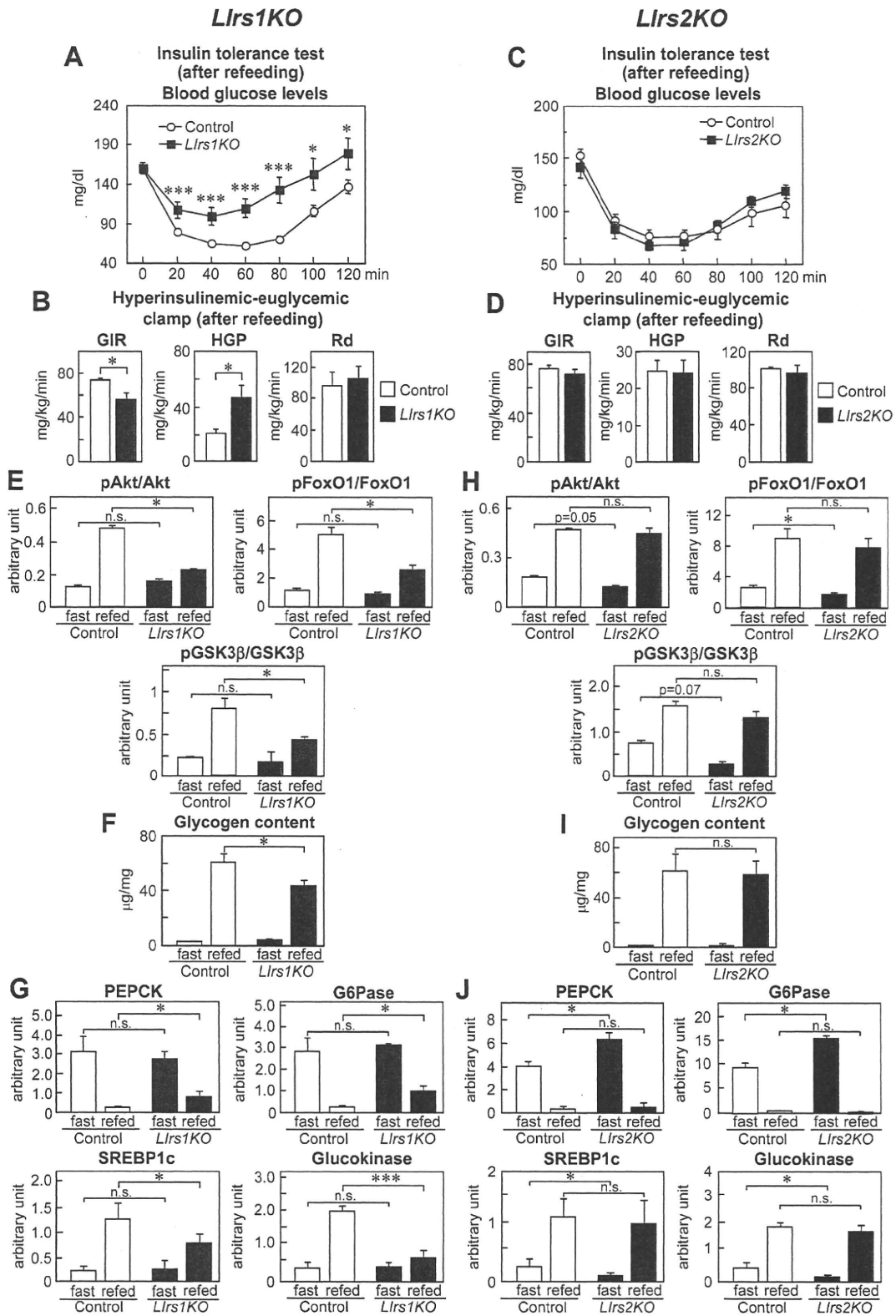
as compared with those in the control mice under the fasting condition, suppression of these expressions after refeeding was significantly impaired in the *LIrs1KO* mice as compared with that in the control mice (Figure 3G, upper panels). While the expression levels of SREBP1c and glucokinase were indistinguishable between the control and *LIrs1KO* mice under the fasting condition, these expressions were significantly lower in the *LIrs1KO* mice as compared with the levels in the control mice under the refeeding condition (Figure 3G, lower panels). While reduced phosphorylation of Akt, FoxO1, and GSK3β was observed in the *LIrs2KO* mice under the fasting condition, no such reduction of phosphorylation was observed under the refeeding condition (Figures 3H and S5B). The hepatic glycogen content was also similar between the control and *LIrs2KO* mice under the refeeding condition (Figure 3I). Although the expression levels of PEPCK and G6Pase were significantly higher in the *LIrs2KO* mice than in the control mice under the fasting condition, suppression of these expressions under the refeeding condition was similar in degree to that noted in the control mice under the refeeding condition (Figure 3J, upper panels). The expression levels of SREBP1c and glucokinase were significantly lower in the *LIrs2KO* mice under the fasting condition; however, these expressions were restored to levels similar to those in the control mice under the refeeding condition (Figure 3J, lower panels). These findings suggest that in the liver, lack of Irs1 affects insulin signaling under the refeeding condition, and lack of Irs2 affects insulin signaling under the fasting condition. In the skeletal muscle (Figure S5C) and white adipose tissue (Figure S5D), the phosphorylation level of Akt was similar between the control and *LIrs1KO* mice or between the control and *LIrs2KO* mice under both the fasting and refeeding conditions. This indicates that insulin signaling was not impaired in the skeletal muscle and white adipose tissue of the *LIrs1KO* and *LIrs2KO* mice under either the fasting or the refeeding condition.

Distinct Roles of Irs1 and Irs2 in Mediating the Actions of Insulin in the Liver

What are the reasons for these differences between the *LIrs1KO* and *LIrs2KO* mice? We examined the expressions of Irs1, Irs2, and the PI3K activity associated with Irs1 and Irs2 under the fasting and refeeding conditions. The Irs1 mRNA and protein levels remained unchanged at 6 hr after the start of refeeding following the 24 hr fasting, which is associated with an ~5-fold increase of the Irs1-associated PI3K activity under the refeeding condition (Figure 4A). In contrast, the Irs2 mRNA and protein levels were significantly decreased after refeeding, associated with Irs2-associated PI3K activity that was not increased even under the

refeeding condition (Figure 4B). We next examined in greater detail the diurnal changes in the glucose and insulin levels, the expressions of Irs1 and Irs2, and their downstream molecules under the fasting and refeeding conditions in the control, *LIrs1KO*, and *LIrs2KO* mice. The blood glucose levels were almost indistinguishable between the control and *LIrs1KO* mice or between the control and *LIrs2KO* mice throughout the experiment (Figure 5A, upper panels). In contrast, the *LIrs1KO* mice exhibited higher serum insulin levels at 4 and 6 hr after the start of refeeding than the control mice (Figure 5A, lower-left panel), the *LIrs2KO* mice exhibited higher serum insulin levels after the 24 hr fasting and at 30 and 60 min after the start of refeeding than the control mice (Figure 5A, lower-right panel). The mRNA levels of *Irs1* were slightly increased during the second half of the 24 hr fasting and remained essentially unaltered after refeeding in both the control and *LIrs2KO* mice (Figure 5B, upper panel). The mRNA levels of *Irs2* were markedly increased during the second half of the 24 hr fasting, and then fell immediately after the start of refeeding in both the control and *LIrs1KO* mice (Figure 5B, lower panel). Although the *Irs2* mRNA expression after refeeding remained suppressed in the control mice, the Irs2 expression in the *LIrs1KO* mice began to increase by 2 hr after the start of refeeding (Figure 5B, lower panel). The Irs1 protein levels remained essentially unaffected by food intake throughout the experiment, which is associated with a mobility shift from 30 min until 4 hr after refeeding in the control mice (Figure 5C). The Irs2 protein levels increased during the 24 hr fasting in the control mice (Figure 5C). The Irs2 protein underwent a prominent mobility shift immediately after the start of refeeding, presumably due to insulin-stimulated tyrosine phosphorylation (Figure 5C). The Irs2 protein levels rapidly decreased after refeeding (Figure 5C). Recruitment of the p85-adaptor subunit of PI3K to Irs1 immunoprecipitates (Figure S6A, left panels) and the PI3K activity associated with Irs1 (Figures 5D, upper-left panel, and S6B, upper panel) began to increase by 2 hr after the start of refeeding. In contrast, recruitment of the p85-adaptor subunit of PI3K to Irs2 immunoprecipitates (Figure S6A, right panels) and the PI3K activity associated with Irs2 (Figures 5D, lower-left panel, and S6B, lower panel) increased during the second half of the 24 hr fasting, despite the decrease in the serum insulin levels, and increased further up to 30 min after the start of refeeding, before decreasing rapidly thereafter. These data suggest that Irs2 mainly acts during fasting and immediately after the start of refeeding, and Irs1 takes over the lead role thereafter. In fact, during fasting or immediately after the start of refeeding, while the PI3K activity associated with Irs2 (Figures 5D, lower-right panel, and S6C, upper panel) and with

---

Figure 3. *LIrs1KO* (but Not *LIrs2KO*) Mice Exhibited Insulin Resistance under the Refeeding Condition

(A) ITT in the control and *LIrs1KO* mice at 6 hr after the start of refeeding following 24 hr fasting (n = 17–23).

(B) Hyperinsulinemic-euglycemic clamp study in the control and *LIrs1KO* mice at 6 hr after the start of refeeding following 24 hr fasting (n = 5–6).

(C) ITT in the control and *LIrs2KO* mice at 6 hr after the start of refeeding following 24 hr fasting (n = 10–20).

(D) Hyperinsulinemic-euglycemic clamp study in the control and *LIrs2KO* mice at 6 hr after the start of refeeding following 24 hr fasting (n = 6–10).

(E–G) Phosphorylation of Akt, FoxO1, and GSK3β in the liver (E), the hepatic glycogen content (F), and the expression levels of PEPCK, G6Pase, SREBP1c, and glucokinase in the liver (G) of the control and *LIrs1KO* mice after 24 hr fasting or at 6 hr after the start of refeeding following 24 hr fasting (F and G, n = 5–6). In (E), results are representative of three independent experiments.

(H–J) Insulin-stimulated phosphorylation of Akt, FoxO1, and GSK3β in the liver (H), the hepatic glycogen content (I), and the expression levels of PEPCK, G6Pase, SREBP1c, and glucokinase in the liver (J) of the control and *LIrs2KO* mice after 24 hr fasting or at 6 hr after the start of refeeding following 24 hr fasting (I and J, n = 6–10). In (H), results are representative of three independent experiments. All the experiments illustrated in this figure were performed using 8- to 10-week-old male mice. Results are represented as mean ± SEM *p < 0.05, ***p < 0.001.
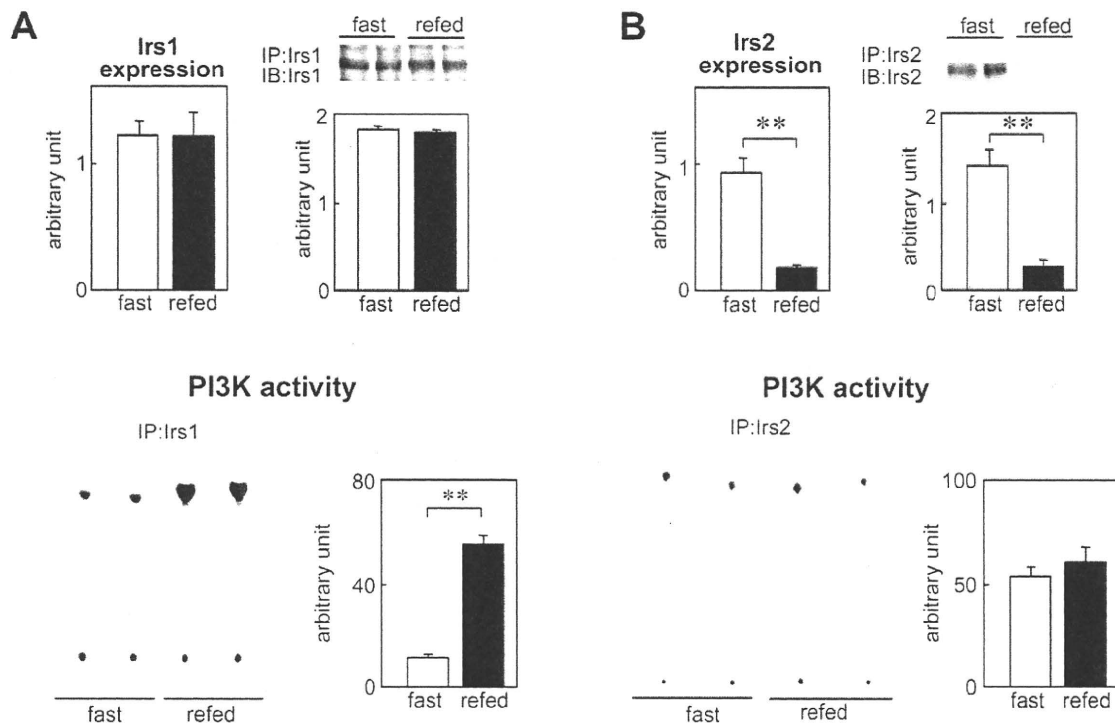
Figure 4. Expressions of Irs1 and Irs2, and the PI3K Activity Associated with Irs1 and Irs2 under the Fasting and Refeeding Conditions
(A and B) Irs1 mRNA and protein levels and Irs1-associated PI3K activity (A), and Irs2 mRNA and protein levels and Irs2-associated PI3K activity (B) in the liver of the control mice after 24 hr fasting or at 6 hr after the start of refeeding following 24 hr fasting (n = 6). The results of western blotting and the PI3K activity are representative of three independent experiments.
All the experiments illustrated in this figure were performed using 8- to 10-week-old male mice. Results are represented as mean ± SEM **p < 0.01.

tyrosine-phosphorylated proteins (Figure S6C, lower panels) increased in the *LIrs1KO* mice, the PI3K activity associated with Irs1 (Figures 5D, upper-right panel and S6D, upper panel) and with tyrosine-phosphorylated proteins (Figure S6D, lower panels) did not increase in the *LIrs2KO* mice. However, the PI3K activity associated with Irs1 (Figures 5D, upper-right panel, and S6D, upper panel) and with tyrosine-phosphorylated proteins (Figure S6D, lower panels) in the *LIrs2KO* mice began to increase by 2 hr after the start of refeeding, while the PI3K activity associated with Irs2 (Figures 5D, lower-right panel, and S6C, upper panel) and with tyrosine-phosphorylated proteins (Figure S6C, lower panels) in the *LIrs1KO* mice rather decreased after refeeding. Consistent with this, Akt phosphorylation was induced immediately after the start of refeeding in the *LIrs1KO* mice (Figure S6E), but not in the *LIrs2KO* mice (Figure S6F). Akt phosphorylation in the *LIrs2KO* mice began to increase by 2 hr after the start of refeeding (Figure S6F), but this Akt phosphorylation in the *LIrs1KO* mice rather decreased after refeeding (Figure S6E). Thus, Akt phosphorylation decreased during fasting and was induced immediately after the start of refeeding, and this induction was sustained for at least 6 hr after the start of refeeding in the control mice (Figures 5E and S6G). These data and the phenotypes observed in the *LIrs1KO* and *LIrs2KO* mice suggest that Irs2 mainly functions under the fasting condition and for a short period immediately after the start of refeeding; Irs1 primarily acts thereafter, under the refeeding condition,

suggesting the existence of a functional relay between Irs1 and Irs2 in insulin signaling during fasting and after refeeding.

LIrs1/2DKO Mice Developed Diabetes and Exhibited Insulin Resistance

In order to determine whether abrogation of both Irs1 and Irs2 in the liver may cause insulin resistance under both the fasting and refeeding conditions, we generated *LIrs1/2DKO* mice. While the *Irs1* and *Irs2* alleles were not detected in the livers, both continued to be expressed in all of the other tissues than the livers of the *LIrs1/2DKO* mice (Figure S7A). The expressions of both *Irs1* and *Irs2* mRNA (Figure S7B) and protein (Figure 6A, upper panels) were almost completely abrogated in the livers of the *LIrs1/2DKO* mice. Insulin-stimulated tyrosine phosphorylation of Irs1 and Irs2 (Figure 6A, lower panels) and recruitment of the p85-adaptor subunit of PI3K to the Irs1 or Irs2 immunoprecipitates (Figure S7C) were also abrogated in the fasted *LIrs1/2DKO* mice. Insulin-stimulated PI3K activity associated with Irs1 (Figure 6B, left panel), Irs2 (Figure 6B, middle panel), and tyrosine-phosphorylated proteins (Figure 6B, right panel) was almost completely abrogated in the liver of the fasted *LIrs1/2DKO* mice. Insulin-stimulated phosphorylation of Akt, FoxO1, and GSK3β was also almost completely abrogated in these fasted mice (Figures 6C and S7D), suggesting that insulin signaling is almost completely mediated by Irs1 and Irs2 in the liver under the fasting condition. The *LIrs1/2DKO* mice showed

similar body-weight gain to the control mice (data not shown). An ITT after fasting in 8-week-old *LIrs1/2DKO* mice revealed severe insulin resistance (Figure 6D), and an OGTT conducted after fasting in these mice revealed severe glucose intolerance with marked hyperinsulinemia (Figure 6E), indicating that *LIrs1/2DKO* mice developed diabetes. These phenotypes were similar to those of the *LIRKO* mice (Michael et al., 2000), suggesting that insulin-receptor signaling may be almost exclusively mediated by Irs1 and Irs2 in the liver. However, while the glucose tolerance gradually improved by the age of 24 weeks in the *LIRKO* mice (Michael et al., 2000), the severe insulin resistance (Figure 6F) and glucose intolerance (Figure 6G) persisted in the *LIrs1/2DKO* mice until 24 weeks of age. Consistent with the results of the ITT, the GIR and R_d were significantly lower (and the HGP significantly higher) in the *LIrs1/2DKO* mice under the fasting condition (Figure 6H). The serum levels of TC, TG, and FFA were not significantly different between the control and *LIrs1/2DKO* mice under the fasting condition (Figure 6I). The serum leptin and adiponectin levels, however, were significantly higher in the *LIrs1/2DKO* mice than in the control mice under the fasting condition (Figure 6J). The TG content in the liver was not significantly different between the control and *LIrs1/2DKO* mice under the nonfasted condition (Figure 6K).

Unlike the *LIrs1KO* or *LIrs2KO* mice, the degree of insulin resistance remained unchanged even after refeeding in the *LIrs1/2DKO* mice (Figure 7A). Consistent with the results of the ITT, the GIR and R_d were significantly lower (and the HGP significantly higher) in the *LIrs1/2DKO* mice under the refeeding condition (Figure 7B). Moreover, phosphorylation of Akt, FoxO1, and GSK3β remained almost completely abrogated in the *LIrs1/2DKO* mice under the refeeding condition (Figure 7C). The hepatic glycogen content in the *LIrs1/2DKO* mice was significantly lower than that in the control mice under the refeeding condition—although it was increased as compared with that noted under the fasting condition (Figure 7D)—despite the absence of GSK3β phosphorylation (Figure 7C). While the PEPCK and G6Pase expressions were increased in the *LIrs2KO* mice under the fasting condition (Figure 3J), unexpectedly, their expression levels were similar in the control and *LIrs1/2DKO* mice (Figure 7E). This may be explained by the suppression of hepatic gluconeogenesis via the hypothalamus induced by the marked hyperinsulinemia (Obici et al., 2002b). Suppression of PEPCK and G6Pase expressions under the refeeding condition was significantly impaired in the *LIrs1/2DKO* mice (Figure 7E). The expression level of SREBP1c was similar between the control and *LIrs1/2DKO* mice under the fasting condition, but was significantly decreased under the refeeding condition in the *LIrs1/2DKO* mice as compared with that in the control mice (Figure 7E). The expression of glucokinase was almost completely abrogated in the *LIrs1/2DKO* mice under both the fasting and refeeding conditions (Figure 7E). These findings indicate that the *LIrs1/2DKO* mice showed insulin resistance under both the fasting and refeeding conditions.

Hepatic Overexpression of Dominant-Negative FoxO1-Ameliorated Diabetes in the *LIrs1/2DKO* Mice

FoxO1 is a forkhead winged/helix transcription factor that mediates many effects of insulin downstream of the Irs-PI3K-Akt cascade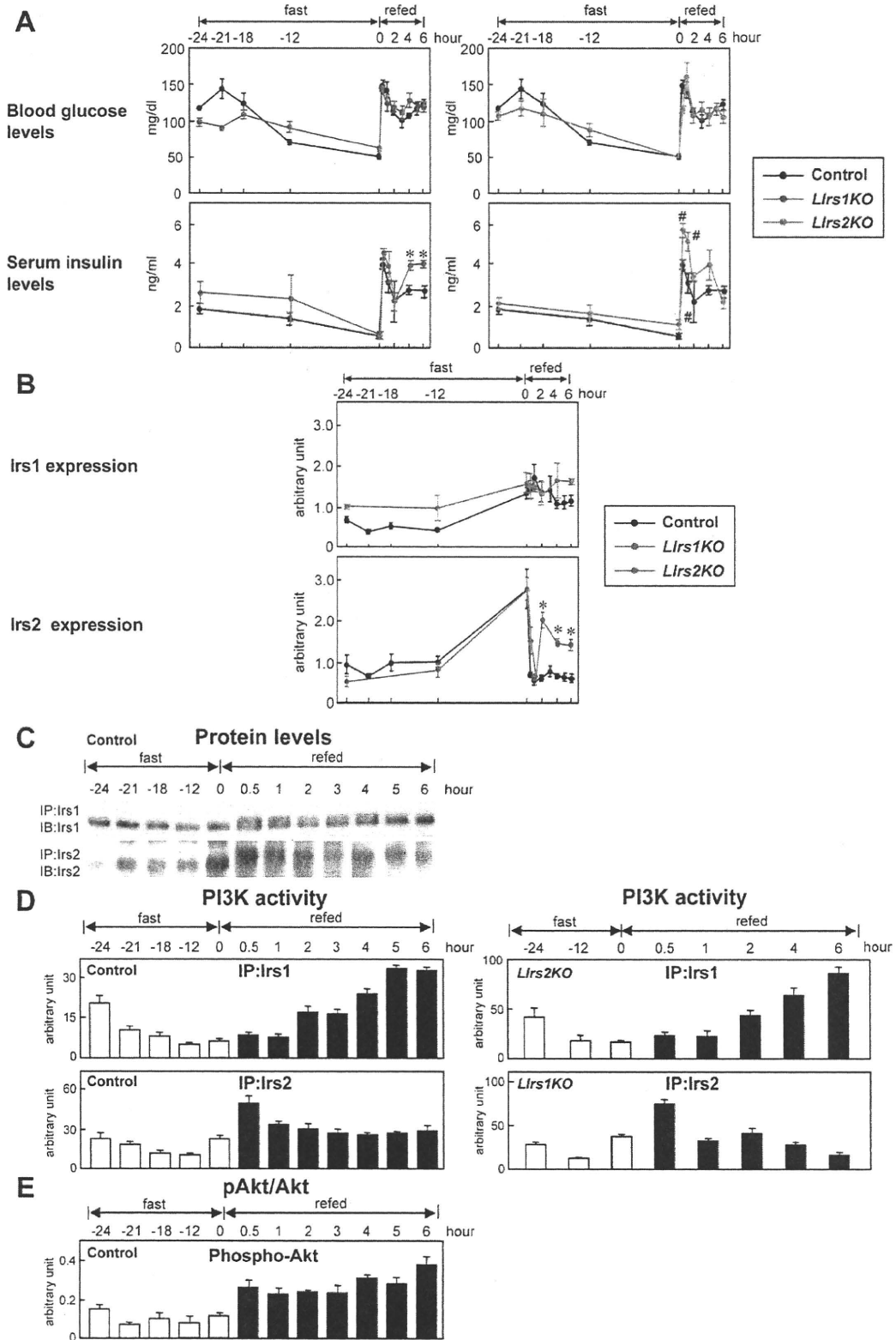 (Nakae et al., 1999; Kops et al., 1999; Brunet et al., 1999). In mammals, nuclear FoxO1, which accumulates in the presence of insulin resistance, dysregulates nutrient homeostasis by promoting hepatic gluconeogenesis, while the suppression of FoxO1 expression has been demonstrated to reverse the effects of insulin resistance and restore glucose tolerance in diabetic mice (Altomonte et al., 2003; Taniguchi et al., 2006). Thus, in order to investigate whether FoxO1 mediates insulin-induced regulation of glucose homeostasis downstream of Irs1 and Irs2 in the liver, expression of dominant-negative FoxO1 (DN-FoxO1) (Nakae et al., 2001) was induced in the livers of the *LIrs1/2DKO* mice. The blood glucose and serum insulin levels before and after glucose loading were partially, but significantly, decreased during an OGTT conducted after fasting in the *LIrs1/2DKO* mice treated with DN-FoxO1, as compared with the levels in the *LIrs1/2DKO* mice treated with lacZ (Figure 7F). These findings suggest that the Irs1/Irs2-FoxO1 pathway may play an important role in the regulation of glucose homeostasis in the liver under the fasting condition.

DISCUSSION

The liver maintains blood glucose levels within a normal range: while it ensures a sufficient supply of glucose in the fasting state, it takes up ingested carbohydrate to store it as glycogen and synthesizes lipids in the fed state, although this dual nature has not been fully accounted for in terms of insulin signaling. In this study, the *LIrs1KO* mice failed to exhibit insulin resistance during fasting, but showed insulin resistance after refeeding, associated with decreased expressions of glucokinase and SREBP1c. Conversely, the *LIrs2KO* mice exhibited insulin resistance during fasting but not after refeeding, associated with increased expression of PEPCK and G6Pase. These data suggest that both Irs1 and Irs2 are physiologically required for diurnal regulation of glucose metabolism by insulin in the liver.

Our close monitoring of the diurnal changes of glucose and insulin levels revealed that although the blood glucose levels were almost indistinguishable between the *LIrs1KO* and *LIrs2KO* mice (Figure 5A, upper panels), the *LIrs1KO* mice exhibited higher serum insulin levels at 4 and 6 hr after the start of refeeding. The *LIrs2KO* mice exhibited higher serum insulin levels after the 24 hr fasting and at 30 and 60 min after the start of refeeding than the control mice (Figure 5A, lower panels). These results indicate the presence of insulin resistance at these time points, which was confirmed by the results of the ITT and hyperinsulinemic-euglycemic clamp studies in the *LIrs1KO* mice under the refeeding condition (Figures 3A and 3B) and the *LIrs2KO* mice under the fasting condition (Figures 2D and 2F).

Insulin has been shown to suppress the expression of Irs2 both in vitro and in vivo, by inhibiting the synthesis of *Irs2* mRNA at the transcriptional level (Zhang et al., 2001; Hirashima et al., 2003; Taniguchi et al., 2006). Indeed, the mRNA levels of *Irs2* in the control mice increased during the second half of the 24 hr fasting—when the serum insulin levels were quite low—and immediately decreased within 30 min after the start of refeeding, which is associated with increase of the serum insulin levels induced by the food intake (Figures 5A and 5B). Our results strongly suggest that suppression of Irs2 immediately after the start of refeeding, presumably due to the increased serum insulin levels, may be mediated by Irs2 itself, because PI3K activity

A

Blood glucose levels

Serum insulin levels

Control
LIrs1KO
LIrs2KO

B

Irs1 expression

Irs2 expression

Control
LIrs1KO
LIrs2KO

C **Protein levels**

Control

fast   refed
-24 -21 -18 -12 0 0.5 1 2 3 4 5 6 hour

IP:Irs1
IB:Irs1

IP:Irs2
IB:Irs2

D **PI3K activity**   **PI3K activity**

Control   IP:Irs1

Control   IP:Irs2

LIrs2KO   IP:Irs1

LIrs1KO   IP:Irs2

E **pAkt/Akt**

Control   Phospho-Akt

associated with Irs2— but not Irs1—increased immediately after the start of refeeding not only in the control mice, but also in the *LIrs1KO* mice (Figures 5C, S6B, S6C, and S6D). Downregulation of Irs2 expression by Irs2 itself implies the existence of a feedback mechanism to prevent excessive insulin-signal transmission by Irs2 in response to food intake. Whereas the sharp fall of the *Irs2* mRNA levels in the control mice persisted immediately after the start of refeeding, the levels in the *LIrs1KO* mice began to increase again at 2 hr after the start of refeeding (Figure 5B). This suggests that Irs1, as well as Irs2, is required for the suppression of *Irs2* mRNA after the start of refeeding.

Expression of a sufficient amount of hepatic Irs2 during fasting appears to be pivotal for normal glucose homeostasis. If Irs2 protein is abundantly expressed during fasting, elevated glucose levels promptly decrease after refeeding. However, in the presence of hyperinsulinemia with insulin resistance (when the fasting Irs2 level is scarce), insulin signaling is impaired, and the elevated glucose levels fail to decrease immediately after the start of refeeding. In fact, *LIrs2KO* mice showed glucose intolerance (Figure 2E), while the *LIrs1KO* mice exhibited no such glucose intolerance (Figure 2B).

Based on our findings, we propose that glucose homeostasis is regulated by both hepatic Irs1 and Irs2; Irs1 and Irs2 exert distinct actions under the fasting and refeeding conditions. The serum insulin levels decrease gradually during fasting and increase immediately after the start of refeeding. Irs2 protein levels increase during the second half of a fasting period and decrease immediately after the start of refeeding, while the Irs1 protein levels remain essentially unaffected by food intake. The PI3K activity associated with Irs2 begins to increase during the second half of a fasting period despite the decrease in serum insulin levels and reaches its peak immediately after the start of refeeding, before rapidly decreasing thereafter. On the other hand, the PI3K activity associated with Irs1 begins to increase by a few hours after the start of refeeding and reaches its peak thereafter, suggesting a dynamic switch of the principal effector in the hepatic insulin signaling during fasting and after refeeding. Thus, we propose the concept of the existence of a functional relay between Irs1 and Irs2 in hepatic insulin signaling during fasting and after refeeding; Irs1 functions primarily after refeeding and Irs2 functions mainly during fasting and immediately after the start of refeeding. This also indicates that Irs2 may be the main contributor to the regulation of gluconeogenesis, i.e., PEPCK and G6Pase, while Irs1 may predominantly regulate the expression of SREBP1c and glucokinase.

This concept could explain most (if not all) of the findings of previous studies on the roles of Irs1 and Irs2 in the regulation of glucose and lipid metabolism by insulin both in vitro and in vivo. With respect to Irs1-dependent signals, Kasuga and colleagues argued that the Irs1-PI3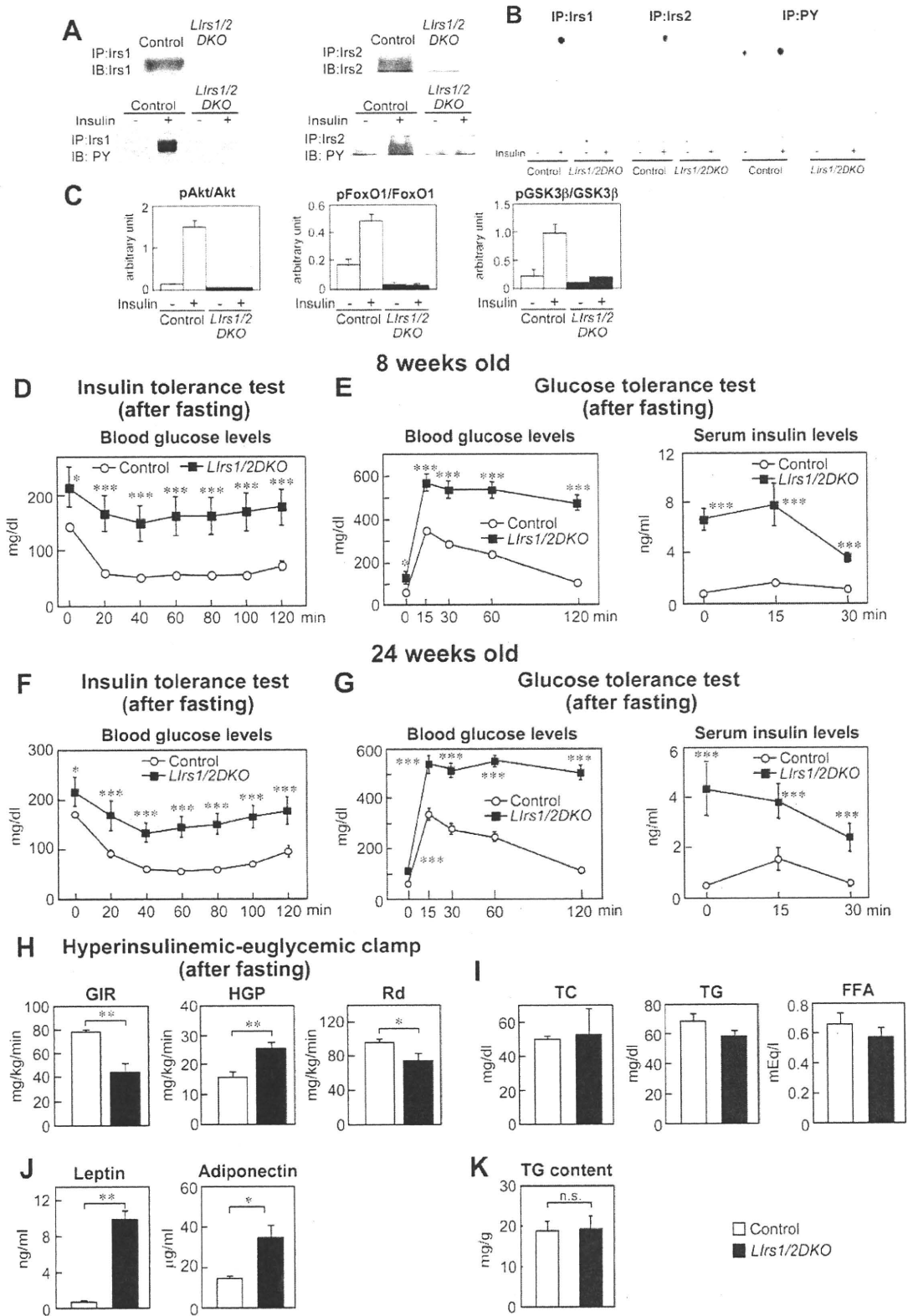K pathway is essential for the insulin-induced expression of the SREBP1c and glucokinase genes in cultured-rat hepatocytes (Matsumoto et al., 2002). The group led by Kahn has proposed that acute suppression of hepatic Irs1 by adenovirus-mediated short hairpin RNA (shRNA) results in decreased expression of glucokinase induced by insulin (Taniguchi et al., 2005). With respect to Irs2-dependent pathways, Dong et al. reported that the fasted *LIrs2KO* mice in their study exhibited glucose intolerance and that the expression of PEPCK increased under the fasting condition (Dong et al., 2006).

On the other hand, it is likely that distinct compensatory mechanisms are induced by genetic ablation or relatively acute shRNA-mediated inactivation, giving rise to the phenotypic differences (Michael et al., 2000; Taniguchi et al., 2005). Indeed, chronic, complete shutdown of insulin signaling in the livers of the *LIRKO* mice results in decreased serum TG levels but no alteration of lipid accumulation in the liver (Michael et al., 2000), whereas double knockdown of Irs1 and Irs2 by shRNA treatment results in increased TG levels in the serum and liver (Taniguchi et al., 2005), shown by the same group. Thus, the phenotype in regard to the lipid synthesis in the liver of the *LIrs1/2DKO* mice is indeed more consistent with that of the *LIRKO* mice, and it is possible that incomplete inactivation of Irs proteins may enhance some of the insulin actions and/or promote the shift of substrates for energy storage from glucose to lipids, leading to upregulation of SREBP1c.

Although the serum levels of TC, TG, and FFA were not significantly different between the control and *LIrs1/2DKO* mice, the serum leptin and adiponectin levels were significantly higher in the *LIrs1/2DKO* mice under the fasting condition (Figure 6J), as observed in the *LIRKO* (Cohen et al., 2007) and Irs1/Irs2 double-knockdown mice treated with shRNA (Taniguchi et al., 2005). Recently, it has been reported that the expression levels of the short (Ob-Ra), long (Ob-Rb), and soluble (Ob-Re) forms of the leptin receptor were significantly increased in the liver of the *LIRKO* mice and that insulin suppressed the leptin-receptor expression in isolated hepatocytes from normal mice, suggesting that high levels of circulating leptin receptor bind to leptin and alter its clearance (Cohen et al., 2007). Thus, insulin signaling in the liver plays an important role in leptin homeostasis. Consistent with this, it has been reported that leptin-receptor expression was significantly increased in the livers of the liver-specific Irs2:total Irs-1-knockout mice (Dong et al., 2006) and our *LIrs1/2DKO* mice (data not shown). In contrast, the expressions of adiponectin receptors (AdipoR1 and AdipoR2 [Yamauchi et al., 2003]) were not increased in the livers of the *LIrs1/2DKO* mice (data not shown), suggesting the absence of a significant change in the adiponectin clearance. The molecular mechanism underlying the increase of the serum adiponectin levels in these mice remains unknown.

Figure 5. Distinct Roles of Irs1 and Irs2 in Insulin Signaling in the Liver under the Fasting and Refeeding Conditions

(A and B) Blood glucose and serum insulin levels (A) and the mRNA levels of *Irs1* and *Irs2* (B) in the control (black), *LIrs1KO* (red), and *LIrs2KO* (blue) mice under the fasting and refeeding conditions (n = 4). Results are represented as mean ± SEM *p < 0.05, *LIrs1KO* versus control mice. #p < 0.05, *LIrs2KO* versus control mice.

(C) Protein levels of Irs1 and Irs2 in the liver of the control mice under the fasting and refeeding conditions. Results are representative of three independent experiments.

(D) PI3K activity associated with Irs1 or Irs2 in the control, *LIrs1KO*, and *LIrs2KO* mice under the fasting and refeeding conditions. Results are representative of three independent experiments.

(E) Phosphorylation of Akt in the liver of the control mice under the fasting and refeeding conditions. Results are representative of three independent experiments.

All the experiments illustrated in this figure were performed using 8- to 10-week-old male mice.

A

IP:Irs1 / IB:Irs1 — Control — Llrs1/2 DKO

Insulin − + − + / IP:Irs1 / IB: PY — Control — Llrs1/2 DKO

IP:Irs2 / IB:Irs2 — Control — Llrs1/2 DKO

Insulin − + − + / IP:Irs2 / IB: PY — Control — Llrs1/2 DKO

B IP:Irs1   IP:Irs2   IP:PY

Insulin − + − + / − + − + / − + − +

Control Llrs1/2DKO Control Llrs1/2DKO Control Llrs1/2DKO

C pAkt/Akt   pFoxO1/FoxO1   pGSK3β/GSK3β

arbitrary unit — Insulin − + − + — Control Llrs1/2 DKO

8 weeks old

D Insulin tolerance test (after fasting)

Blood glucose levels — Control / Llrs1/2DKO

E Glucose tolerance test (after fasting)

Blood glucose levels — Control / Llrs1/2DKO

Serum insulin levels — Control / Llrs1/2DKO

24 weeks old

F Insulin tolerance test (after fasting)

Blood glucose levels — Control / Llrs1/2DKO

G Glucose tolerance test (after fasting)

Blood glucose levels — Control / Llrs1/2DKO

Serum insulin levels — Control / Llrs1/2DKO

H Hyperinsulinemic-euglycemic clamp (after fasting)

GIR   HGP   Rd

I TC   TG   FFA

J Leptin   Adiponectin

K TG content

☐ Control
■ Llrs1/2DKO

Why do hepatic Irs1 and Irs2 have distinct roles? One of the reasons may be the dual aspects of the role played by the liver. While other target tissues of insulin simply take in glucose, the liver produces and consumes glucose to adapt to various physiological conditions. The opposing functions of utilizing glucose, that is, glucose production during fasting and glucose uptake after food intake, may be the reason for the distinctive roles of Irs1 and Irs2. In the long history of evolution, mammals had to survive for certain periods without food. The necessity of development of a mechanism to handle sporadic starvation may have resulted in the refined roles of Irs1 and Irs2 under the fasting and refeeding conditions.

In conclusion, Irs1 and Irs2 exert distinct actions under the fasting and refeeding conditions and are almost exclusively responsible for the mediation of insulin signaling in the liver. Understanding the molecular basis of hepatic insulin signaling in the regulation of glucose metabolism may be expected to provide a basis for a better understanding of the pathogenesis and treatment of type 2 diabetes mellitus.

EXPERIMENTAL PROCEDURES

Construction of the Targeting Vector, ES Cell Culture, and Generation of the Mutant Mice

To construct the targeting vector for the *Irs1* gene, a mouse genomic DNA library packaged in Lambda DASH II (Clontech, Mountain View, CA) was screened using mouse *Irs1* cDNA as the probe. Five clones containing the *Irs1* gene were isolated. We constructed a targeting vector in which a third loxP site was introduced into the 5′ side of the *Irs1* gene and the floxed neomycin-resistance gene (*neoR*) was introduced into the 3′ side of the *Irs1* gene (Figure S8A). The diphtheria toxin A fragment (DTA) gene under an MC1 promoter was ligated onto the 5′ end of the homologous region for negative selection against random integration (Kubota et al., 2004). The targeting vector was electroporated into E14.1 embryonic stem cells (129/Sv), and the cells were screened for homologous recombinant clones by Southern blot analysis using probe A and probe B, as described previously (Kubota et al., 2004) (Figures S8A and S8B). The cells were aggregated with eight-cell embryos from ICR mice and transferred into pseudopregnant ICR females to generate chimeric mice. Male chimeric mice with an agouti coat color were mated with C57Bl/6 female mice to generate heterozygous (*Irs1*$^{lox/+}$) mice (Kubota et al., 2004).

Animals

The mice were housed under a 12 hr light-dark cycle and given regular chow, CE-2 (CLEA Japan, Inc., Tokyo, Japan), consisting of 25.6% (w/w) protein, 3.8% fiber, 6.9% ash, 50.5% carbohydrates, 4% fat, and 9.2% water. Albu-
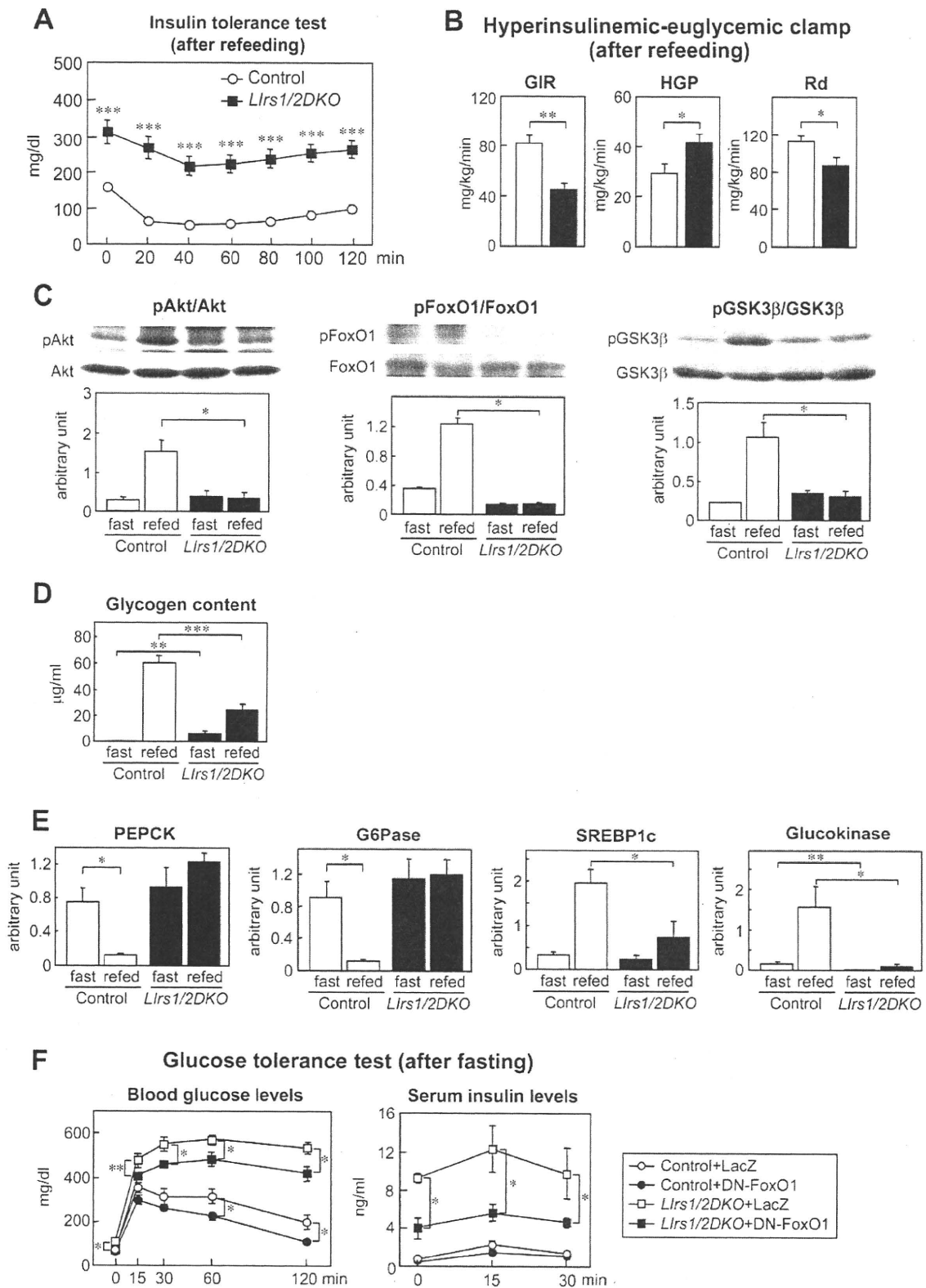
min-Cre-recombinase transgenic mice (*AlbCre* mice) were purchased from Jackson Laboratory. The *Irs1*$^{lox/+}$ mice or mice with a floxed allele of *Irs2* (*Irs2*$^{lox/lox}$) (Kubota et al., 2004) were intercrossed with the *AlbCre* mice to generate *AlbCreIrs1*$^{lox/+}$ or *AlbCreIrs2*$^{lox/+}$ mice. *AlbCreIrs1*$^{lox/+}$ or *AlbCreIrs2*$^{lox/+}$ mice were crossed with *Irs1*$^{lox/+}$ or *Irs2*$^{lox/+}$ mice to obtain wild-type, *Irs1*$^{lox/+}$, *AlbCre*, and *AlbCreIrs1*$^{lox/lox}$ (*LIrs1KO*) mice; or wild-type, *Irs2*$^{lox/+}$, *AlbCre*, and *AlbCreIrs2*$^{lox/lox}$ (*LIrs2KO*) mice, respectively. To generate liver-specific Irs1/Irs2 double-knockout (*LIrs1/2DKO*) mice, *AlbCreIrs1*$^{lox/+}$ or *AlbCreIrs2*$^{lox/+}$ mice were crossed with *Irs2*$^{lox/+}$ or *Irs1*$^{lox/+}$ mice, then the resultant *AlbCreIrs1*$^{lox/+}$/*Irs2*$^{lox/+}$ were crossed with *Irs1*$^{lox/+}$/*Irs2*$^{lox/+}$ mice. The wild-type, *AlbCre*, *Irs1*$^{lox/lox}$, *Irs2*$^{lox/lox}$, and *Irs1*$^{lox/lox}$/*Irs2*$^{lox/lox}$ mice were phenotypically indistinguishable; the *Irs1*$^{lox/lox}$, *Irs2*$^{lox/lox}$, and *Irs1*$^{lox/lox}$/*Irs2*$^{lox/lox}$ mice were used as controls. All the mouse lines were maintained on a mixed background derived from C57Bl/6 and 129/Sv. All experiments in this study were performed using male littermates. For the refeeding condition, the mice were first deprived of food for 24 hr, followed by refeeding for 6 hr before the experiments. Genotyping was performed by PCR amplification of the tail DNA from each mouse at 3 weeks of age. The PCR primers for the Cre recombinase were 5′-ACATGTTCAGGGATCGCCAGG-3′ and 5′-TAACCAGTGAAACAGCATTG C-3′. The primers for the *Irs1* and floxed *Irs1* alleles were 5′-TCTGTGAGC CTGTTTTCTGGTGGTC-3′, 5′-TCCTATTGATGAAAGCCCAAGGCAC-3′, and 5′-CAGCGCATCGCCTTCTATCGCCTTC-3′. The primers for the *Irs2* and floxed *Irs2* alleles were 5′-CCAGTGGGTGGCAGTGTGGGTAGG-3′, 5′-CAGC GCATCGCCTTCTATCGCCTTC-3′, and 5′-GCCATGTCCTTACAACCATTAGC GG-3′, respectively. To detect Cre-mediated recombination at the genomic DNA level in various tissues by PCR, primers were designed for the upstream portion (primer a) and downstream portion (primer b) of *Irs1* genomic DNA and the upstream portion (primer c) and downstream portion (primer d) of *Irs2* genomic DNA (Figure S1A). Primer a was 5′-TTTCCTACATAATGCGAGG TCCCC-3′, primer b was 5′-AAATGTTGGAAGCAGAATCAGGACC-3′, primer c was 5′-CCAGTGGGTGGCAGTGTGGGTAAGA-3′, and primer d was 5′-CC CATGTCTGCTTGTATGGAGAGCC-3′. Primer pairs a and b yielded PCR products with a length of 0.2 kb after Cre-mediated Irs1 deletion, and primer pairs c and d yielded PCR products with a length of 0.4 kb after Cre-mediated Irs2 deletion. The primers used for G3PDH were 5′-TGAAGGTCGGTGTGAACG GATTTGGC-3′ and 5′-CATGTAGGCCATGAGGTCCACCAC-3′. The methods used for animal care and the experimental procedures were approved by the Animal Care Committee of the University of Tokyo.

Immunoprecipitation, Western Blot Analysis, and PI3K Assay

For insulin stimulation, 10 or 0.1 U of human insulin (Novolin R, Novo Nordisk, Denmark) were injected via the inferior vena cava; the liver, skeletal muscle or white adipose tissue were dissected and immediately frozen in liquid nitrogen 70 s or 30 min after the insulin stimulation, respectively. To prepare tissue lysates, frozen tissue was homogenized in buffer A (25 mM Tris-HCl [pH 7.4], 10 mM sodium orthovanadate, 10 mM sodium pyrophosphate, 100 mM sodium fluoride, 10 mM EDTA, 10 mM EGTA, and 1 mM phenylmethylsulfonyl fluoride [PMSF]). For immunoprecipitation of Irs1, Irs2, and phosphotyrosine, 5 mg of the liver extracts were incubated with specific antibodies against

---

Figure 6. *LIrs1/2DKO* Mice Showed Severe Insulin Resistance and Developed Diabetes

(A) In upper panels, liver lysates were immunoprecipitated with anti-Irs1 or anti-Irs2 antibody and subsequently immunoblotted with anti-Irs1 or anti-Irs2 antibody in 8- to 10-week-old control and *LIrs1/2DKO* mice. Lower panels show insulin-stimulated tyrosine phosphorylation of Irs1 or Irs2 at 70 s after administration of 10 U of insulin in the liver of the control and *LIrs1/2DKO* mice after overnight (about 16 hr) fasting. Results are representative of three independent experiments.

(B) Insulin-stimulated PI3K activity associated with Irs1, Irs2, and tyrosine-phosphorylated proteins at 70 s after administration of 10 U of insulin in the liver of 8- to 10-week-old control and *LIrs1/2DKO* mice after overnight (about 16 hr) fasting. Results are representative of three independent experiments.

(C) Insulin-stimulated phosphorylation of Akt, FoxO1, and GSK3β at 70 s after administration of 10 U of insulin in the liver of 8- to 10-week-old control and *LIrs1/2DKO* mice after overnight (about 16 hr) fasting. Results are representative of three independent experiments. .

(D) ITT in 8-week-old control and *LIrs1/2DKO* mice after 3 hr fasting (n = 16–19).

(E) Blood glucose and serum insulin levels in 8-week-old control and *LIrs1/2DKO* mice during an OGTT conducted after 24 hr fasting (n = 17–18).

(F) ITT in 24-week-old control and *LIrs1/2DKO* mice after 3 hr fasting (n = 9–17).

(G) Blood glucose and serum insulin levels in 24-week-old control and *LIrs1/2DKO* mice during an OGTT conducted after 24 hr fasting (n = 10–13).

(H) GIR, HGP, and R$_d$ in 8-week-old control and *LIrs1/2DKO* mice in the hyperinsulinemic-euglycemic clamp study conducted after 6 hr fasting (n = 6–7).

(I) Serum levels of TC, TG, and FFA in 8-week-old control and *LIrs1/2DKO* mice after overnight (about 16 hours) fasting (n = 10–14).

(J) Serum leptin and adiponectin levels in 8-week-old control and *LIrs1/2DKO* mice after overnight (about 16 hr) fasting (n = 6–14).

(K) The TG content of the liver in 8-week-old nonfasted control and *LIrs1/2DKO* mice (n = 6). Results are represented as mean ± SEM *p < 0.05. **p < 0.01, ***p < 0.001.

A Insulin tolerance test (after refeeding)

B Hyperinsulinemic-euglycemic clamp (after refeeding)

GIR   HGP   Rd

C

pAkt/Akt   pFoxO1/FoxO1   pGSK3β/GSK3β

D Glycogen content

E

PEPCK   G6Pase   SREBP1c   Glucokinase

F Glucose tolerance test (after fasting)

Blood glucose levels   Serum insulin levels

- Control+LacZ
- Control+DN-FoxO1
- Llrs1/2DKO+LacZ
- Llrs1/2DKO+DN-FoxO1

Irs1, Irs2, or phosphotyrosine, respectively, for 1 hr at 4°C. Then, protein G-Sepharose was added, followed by incubation for 2 hr at 4°C. After washing three times with buffer A, the immunocomplexes were resolved on 7% SDS-PAGE. Phosphorylated or total protein was analyzed by immunoblotting with specific antibodies against Irs1, Irs2, phosphotyrosine, and anti-p85[PAN] antibody. Phosphorylated or total protein of Akt, FoxO1, and Gsk3β were analyzed by immunoblotting with specific antibodies after the tissue lysates were resolved on SDS-PAGE and transferred to a Hybond-P PVDF transfer membrane (Amersham Biosciences, Buckinghamshire, UK). Bound antibodies were detected with HRP-conjugated secondary antibodies, using ECL detection reagents (Amersham Biosciences, Buckinghamshire, UK). For the PI3K assay, 5 mg of the liver extracts were immunoprecipitated with antibody against Irs1, Irs2, or phosphotyrosine, and the immune complexes were assayed for PI3K activity using phosphatidylinositol as the substrate. The procedure was performed as described previously (Kubota et al., 2000). The activities of PI3K were quantitated with an image analyzer (BAS 2000, Fuji Film, Tokyo, Japan) and expressed as the photostimulated luminescence intensity (PSL).

In Vivo Glucose Homeostasis
For the glucose tolerance test, the mice were loaded with oral glucose at 1.5 mg/g body weight. Blood samples were taken at different time points, and the concentrations of glucose were measured with an automatic glucometer (Glutest Ace, Sanwa Chemical Co., Nagoya, Japan). Whole blood was collected and centrifuged in heparinized tubes, and the separated serum samples were stored at −20°C. Insulin levels were determined using an insulin radioimmunoassay (RIA) kit (BIOTRAK, Amersham, UK), with rat insulin as the standard (Kubota et al., 1999). For the insulin tolerance test, mice were intraperitoneally challenged with 0.75 mU/g (body weight) of human insulin (Novolin R, Novo Nordisk, Denmark). Venous blood samples were then drawn at different time points (Kubota et al., 1999).

Hyperinsulinemic-Euglycemic Clamp Study
Clamp studies were carried out as described previously (Kubota et al., 2006), with slight modifications. In brief, 2–3 days before the study, an infusion catheter was inserted into the right jugular vein of the animals under general anesthesia induced with sodium pentobarbital. The studies on the mice were performed under conscious and unstressed conditions. A continuous infusion of insulin (Novolin R, Novo Nordisk, Denmark) was given (5.0 mU/kg/min for the *LIrs1KO* and *LIrs2KO* mice and 7.5 mU/kg/min for the *LIrs1/2DKO* mice), and the blood glucose concentration (monitored every 5 min) was maintained at ~120 mg/dl by administration of glucose (5 g of glucose per 10 ml enriched to approximately 20% with [6,6-2H2]glucose [Sigma]) for 120 min. Blood was sampled via tail-tip bleeds at 90, 105, and 120 min, for determination of the rate of glucose disappearance (R_d). R_d was calculated according to non-steady-state equations, and hepatic glucose production (HGP) was calculated as the difference between the R_d and the exogenous glucose infusion rates (GIR) (Kubota et al., 2006).

Histology and the Glycogen and TG Contents of the Liver
To study the liver histology, the livers were dissected and fixed in buffered neutral formalin (10%). The fixed-tissue blocks were embedded in paraffin. The paraffin sections (5 μm) were stained by the standard H&E staining procedure. The method for measurement of the glycogen content in the liver has been described previously (Lo et al., 1970). In brief, approximately 50 mg of the liver samples were weighed and boiled in 30% KOH saturated with Na2SO4 and 95% ethanol was added to precipitate the glycogen from the alkaline digestate. After cooling on ice, the samples were centrifuged and the glycogen precipitates were dissolved in distilled H_2O. The glycogen concentrations were then read on a spectrophotometer after the addition of 5% phenol and 96%–98% H_2SO_4. For determining the TG content in the liver, the tissue homogenates were extracted with 2:1 (vol/vol) chloroform/methanol. Chloroform/methanol was added to the homogenate, and the mixture was shaken for 15 min. After centrifugation at 14,000 rpm for 10 min, the organic layer was collected. This extraction was repeated three times, and the collected sample was dried and resuspended in 1% Triton X-100/ethanol. The measurement was conducted using Triglyceride E-test Wako (Wako Pure Chemical Industries, Ltd., Osaka, Japan).

SUPPLEMENTAL DATA

Supplemental Data include eight figures and Supplemental Experimental Procedures and can be found at http://www.cellmetabolism.org/cgi/content/full/8/1/49/DC1/.

REFERENCES

Altomonte, J., Richter, A., Harbaran, S., Suriawinata, J., Nakae, J., Thung, S.N., Meseck, M., Accili, D., and Dong, H. (2003). Inhibition of Foxo1 function is associated with improved fasting glycemia in diabetic mice. Am. J. Physiol. Endocrinol. Metab. 285, E718–E728.

Araki, E., Lipes, M.A., Patti, M.E., Bruning, J.C., Haag, B., 3rd, Johnson, R.S., and Kahn, C.R. (1994). Alternative pathway of insulin signalling in mice with targeted disruption of the Irs1 gene. Nature 372, 186–190.

Brunet, A., Bonni, A., Zigmond, M.J., Lin, M.Z., Juo, P., Hu, L.S., Anderson, M.J., Arden, K.C., Blenis, J., and Greenberg, M.E. (1999). Akt promotes cell survival by phosphorylating and inhibiting a Forkhead transcription factor. Cell 96, 857–868.

Figure 7. *LIrs1/2DKO* Mice Exhibited Insulin Resistance Under the Refeeding Condition

(A) ITT in the control and *LIrs1/2DKO* mice at 6 hr after the start of refeeding following 24 hr fasting (n = 14–15).

(B) GIR, HGP, and R_d in control and *LIrs1/2DKO* mice in the hyperinsulinemic-euglycemic clamp study at 6 hr after the start of refeeding following 24 hr fasting (n = 5–6).

(C–E) Phosphorylation of Akt, FoxO1, and GSK3β in the liver (C), the hepatic glycogen content (D), and the expression levels of PEPCK, G6Pase, SREBP1c, and glucokinase in the liver (E) of 8-week-old control and *LIrs1/2DKO* mice after 24 hr fasting or at 6 hr after the start of refeeding following 24 hr fasting (D and E, n = 6). In (C), results are representative of three independent experiments.

(F) Blood glucose and serum insulin levels in the control and *LIrs1/2DKO* mice treated with lacZ or DN-FoxO1 mice during an OGTT conducted after 24 hr fasting (n = 7–10). All the experiments illustrated in this figure were performed using 8- to 10-week-old male mice, unless otherwise specified. Results are represented as mean ± SEM *p < 0.05, **p < 0.01, ***p < 0.001.

Cohen, S.E., Kokkotou, E., Biddinger, S.B., Kondo, T., Gebhardt, R., Kratzsch, J., Mantzoros, C.S., and Kahn, C.R. (2007). High circulating leptin receptors with normal leptin sensitivity in liver-specific insulin receptor knock-out (LIRKO) mice. J. Biol. Chem. *282*, 23672–23678.

Dong, X., Park, S., Lin, X., Copps, K., Yi, X., and White, M.F. (2006). Irs1 and Irs2 signaling is essential for hepatic glucose homeostasis and systemic growth. J. Clin. Invest. *116*, 101–114.

Gribble, F.M. (2005). Metabolism: a higher power for insulin. Nature *434*, 965–966.

Hirashima, Y., Tsuruzoe, K., Kodama, S., Igata, M., Toyonaga, T., Ueki, K., Kahn, C.R., and Araki, E. (2003). Insulin down-regulates insulin receptor substrate-2 expression through the phosphatidylinositol 3-kinase/Akt pathway. J. Endocrinol. *179*, 253–266.

Kasuga, M. (2006). Insulin resistance and pancreatic beta cell failure. J. Clin. Invest. *116*, 1756–1760.

Kops, G.J., de Ruiter, N.D., de Vries-Smits, A.M., Powell, D.R., Bos, J.L., and Burgering, B.M. (1999). Direct control of the Forkhead transcription factor AFX by protein kinase B. Nature *398*, 630–634.

Kubota, N., Terauchi, Y., Miki, H., Tamemoto, H., Yamauchi, T., Komeda, K., Satoh, S., Nakano, R., Ishii, C., Sugiyama, T., et al. (1999). PPAR gamma mediates high-fat diet-induced adipocyte hypertrophy and insulin resistance. Mol. Cell *4*, 597–609.

Kubota, N., Tobe, K., Terauchi, Y., Eto, K., Yamauchi, T., Suzuki, R., Tsubamoto, Y., Komeda, K., Nakano, R., Miki, H., et al. (2000). Disruption of insulin receptor substrate 2 causes type 2 diabetes because of liver insulin resistance and lack of compensatory beta-cell hyperplasia. Diabetes *49*, 1880–1889.

Kubota, N., Terauchi, Y., Tobe, K., Yano, W., Suzuki, R., Ueki, K., Takamoto, I., Satoh, H., Maki, T., Kubota, T., et al. (2004). Insulin receptor substrate 2 plays a crucial role in beta cells and the hypothalamus. J. Clin. Invest. *114*, 917–927.

Kubota, N., Terauchi, Y., Kubota, T., Kumagai, H., Itoh, S., Satoh, H., Yano, W., Ogata, H., Tokuyama, K., Takamoto, I., et al. (2006). Pioglitazone ameliorates insulin resistance and diabetes by both adiponectin-dependent and -independent pathways. J. Biol. Chem. *281*, 8748–8755.

Lo, S., Russell, J.C., and Taylor, A.W. (1970). Determination of glycogen in small tissue samples. J. Appl. Physiol. *28*, 234–236.

Matsumoto, M., Ogawa, W., Teshigawara, K., Inoue, H., Miyake, K., Sakaue, H., and Kasuga, M. (2002). Role of the insulin receptor substrate 1 and phosphatidylinositol 3-kinase signaling pathway in insulin-induced expression of sterol regulatory element binding protein 1c and glucokinase genes in rat hepatocytes. Diabetes *51*, 1672–1680.

Michael, M.D., Kulkarni, R.N., Postic, C., Previs, S.F., Shulman, G.I., Magnuson, M.A., and Kahn, C.R. (2000). Loss of insulin signaling in hepatocytes leads to severe insulin resistance and progressive hepatic dysfunction. Mol. Cell *6*, 87–97.

Nakae, J., Park, B.C., and Accili, D. (1999). Insulin stimulates phosphorylation of the forkhead transcription factor FKHR on serine 253 through a Wortmannin-sensitive pathway. J. Biol. Chem. *274*, 15982–15985.

Nakae, J., Kitamura, T., Silver, D.L., and Accili, D. (2001). The forkhead transcription factor FoxO1 (Fkhr) confers insulin sensitivity onto glucose-6-phosphatase expression. J. Clin. Invest. *108*, 1359–1367.

Nandi, A., Kitamura, Y., Kahn, C.R., and Accili, D. (2004). Mouse models of insulin resistance. Physiol. Rev. *84*, 623–647.

Obici, S., Feng, Z., Karkanias, G., Baskin, D.G., and Rossetti, L. (2002a). Decreasing hypothalamic insulin receptors causes hyperphagia and insulin resistance in rats. Nat. Neurosci. *5*, 566–572.

Obici, S., Zhang, B.B., Karkanias, G., and Rossetti, L. (2002b). Hypothalamic insulin signaling is required for inhibition of glucose production. Nat. Med. *8*, 1376–1382.

Plum, L., Belgardt, B.F., and Bruning, J.C. (2006). Central insulin action in energy and glucose homeostasis. J. Clin. Invest. *116*, 1761–1766.

Previs, S.F., Withers, D.J., Ren, J.M., White, M.F., and Shulman, G.I. (2000). Contrasting effects of Irs-1 versus Irs-2 gene disruption on carbohydrate and lipid metabolism in vivo. J. Biol. Chem. *275*, 38990–38994.

Saltiel, A.R., and Kahn, C.R. (2001). Insulin signalling and the regulation of glucose and lipid metabolism. Nature *414*, 799–806.

Simmgen, M., Knauf, C., Lopez, M., Choudhury, A.I., Charalambous, M., Cantley, J., Bedford, D.C., Claret, M., Iglesias, M.A., Heffron, H., et al. (2006). Liver-specific deletion of insulin receptor substrate 2 does not impair hepatic glucose and lipid metabolism in mice. Diabetologia *49*, 552–561.

Tamemoto, H., Kadowaki, T., Tobe, K., Yagi, T., Sakura, H., Hayakawa, T., Terauchi, Y., Ueki, K., Kaburagi, Y., Satoh, S., et al. (1994). Insulin resistance and growth retardation in mice lacking insulin receptor substrate-1. Nature *372*, 182–186.

Taniguchi, C.M., Ueki, K., and Kahn, R. (2005). Complementary roles of Irs-1 and Irs-2 in the hepatic regulation of metabolism. J. Clin. Invest. *115*, 718–727.

Taniguchi, C.M., Emanuelli, B., and Kahn, C.R. (2006). Critical nodes in signalling pathways: insights into insulin action. Nat. Rev. Mol. Cell Biol. *7*, 85–96.

Thirone, A.C., Huang, C., and Klip, A. (2006). Tissue-specific roles of IRS proteins in insulin signaling and glucose transport. Trends Endocrinol. Metab. *17*, 72–78.

Tobe, K., Tamemoto, H., Yamauchi, T., Aizawa, S., Yazaki, Y., and Kadowaki, T. (1995). Identification of a 190-kDa protein as a novel substrate for the insulin receptor kinase functionally similar to insulin receptor substrate-1. J. Biol. Chem. *270*, 5698–5701.

Tobe, K., Suzuki, R., Aoyama, M., Yamauchi, T., Kamon, J., Kubota, N., Terauchi, Y., Matsui, J., Akanuma, Y., Kimura, S., et al. (2001). Increased expression of the sterol regulatory element-binding protein-1 gene in insulin receptor substrate-2(−/−) mouse liver. J. Biol. Chem. *276*, 38337–38340.

Wada, A., Yokoo, H., Yanagita, T., and Kobayashi, H. (2005). New twist on neuronal insulin receptor signaling in health, disease, and therapeutics. J. Pharmacol. Sci. *99*, 128–143.

Withers, D.J., Gutierrez, J.S., Towery, H., Burks, D.J., Ren, J.M., Previs, S., Zhang, Y., Bernal, D., Pons, S., Shulman, G.I., et al. (1998). Disruption of Irs-2 causes type 2 diabetes in mice. Nature *391*, 900–904.

Yamauchi, T., Tobe, K., Tamemoto, H., Ueki, K., Kaburagi, Y., Yamamoto-Honda, R., Takahashi, Y., Yoshizawa, F., Aizawa, S., Akanuma, Y., et al. (1996). Insulin signalling and insulin actions in the muscles and livers of insulin-resistant, insulin receptor substrate 1-deficient mice. Mol. Cell. Biol. *16*, 3074–3084.

Yamauchi, T., Kamon, J., Ito, Y., Tsuchida, A., Yokomizo, T., Kita, S., Sugiyama, T., Miyagishi, M., Hara, K., Tsunoda, M., et al. (2003). Cloning of adiponectin receptors that mediate antidiabetic metabolic effects. Nature *423*, 762–769.

Zhang, J., Ou, J., Bashmakov, Y., Horton, J.D., Brown, M.S., and Goldstein, J.L. (2001). Insulin inhibits transcription of IRS-2 gene in rat liver through an insulin response element (IRE) that resembles IREs of other insulin-repressed genes. Proc. Natl. Acad. Sci. USA *98*, 3756–3761.

厚生労働科学研究費補助金

肝炎等克服緊急対策研究事業

非アルコール性脂肪性肝疾患の病態解明と診断法、治療法の開発に関する研究

平成 20－22 年度　　総合研究報告書

（第 2 分冊）

研究代表者　　岡上　武

平成 23（2011）年 3 月

厚生労働科学研究費補助金

肝炎等克服緊急対策研究事業

非アルコール性脂肪性肝疾患の病態解明と診断法、治療法の開発に関する研究

平成 20－22 年度　総括・分担研究報告書

（第 2 分冊）

研究代表者　　岡上　武

平成 23（2011）年 3 月

Original Article

Crucial role of impaired Kupffer cell phagocytosis on the decreased Sonazoid-enhanced echogenicity in a liver of a nonalchoholic steatohepatitis rat model

Shohei Yoshikawa,[1] Hiroko Iijima,[1] Masaki Saito,[1] Hironori Tanaka,[1] Hiroyasu Imanishi,[1] Naoki Yoshimoto,[2] Tomohiro Yoshimoto,[3] Shizue Futatsugi-Yumikura,[4] Kenji Nakanishi,[4] Tohru Tsujimura,[5] Takashi Nishigami,[5] Atsushi Kudo,[6] Shigeki Arii[6] and Shuhei Nishiguchi[1]

[1]Division of Hepatobiliary and Pancreatic Diseases, Department of Internal Medicine, Hyogo College of Medicine, [2]Ultrasound Imaging Center, Hyogo College of Medicine, [3]Laboratory of Allergic Diseases, Institute for Advanced Medical Sciences, Hyogo College of Medicine, [4]Department of Immunology and Medical Zoology, Hyogo College of Medicine, [5]Department of Pathology, Hyogo College of Medicine, and [6]Department of Hepatobiliary Pancreatic Surgery, Tokyo Medical and Dental University, Tokyo, Japan

Aims: To evaluate the dynamics of Kupffer cell (KC) phagocytosis by performing both *in vivo* and *in vitro* studies using Sonazoid (GE Healthcare, Oslo) in a rat nonalcoholic steatohepatitis (NASH) model.

Methods: Contrast enhanced ultrasonography (CEUS) was performed on a rat NASH model induced by a methionine choline deficient diet (MCDD) and control rats, and Sonazoid was used to measure the signal intensity in the liver parenchyma. The uptake of Sonazoid by the KCs was observed by intravital microscopy. Their phagocytic capability was evaluated *in vitro* using isolated and cultured KCs. The uptake of fluorescein isothiocyanate (FITC)-labeled latex beads was observed and quantitatively analyzed by flow cytometry.

Results: In the MCDD group, liver parenchymal enhancement was reduced 20 min after the Sonazoid injection.

Microscopic observation of the isolated and cultured KCs revealed that the number of phagocytosed Sonazoid microbubbles was significantly decreased. Confocal laser scanning microscopic (CLSM) observation showed a decrease in the uptake of the latex beads. A decreased phagocytic capacity in the MCDD group was suggested by the quantitative analysis using flow cytometry, as well as by intravital microscopy.

Conclusions: CEUS with Sonazoid is a powerful evaluation tool to diagnose NASH from an early stage of the disease.

Key words: Kupffer cells, nonalcoholic steatohepatitis, phagocytosis, Sonazoid, ultrasound contrast agents.

INTRODUCTION

NONALCOHOLIC FATTY LIVER disease (NAFLD) has been increasing as the incidence of obesity and metabolic syndrome has been rising. Nonalcoholic steatohepatitis (NASH) draws particular attention due to the risk of progression to cirrhosis and hepatocellular carcinoma.[1–3] Liver biopsy has been considered to be the

only way to definitively diagnose NASH[4,5] because diagnosis using imaging modalities is believed to be impossible.[6] In a recent study, magnetic resonance imaging was used for the quantification of the liver fat content and the evaluation of hepatic fibrosis, but it was still inadequate to replace liver biopsy.[7] Liver biopsy is not necessarily recommended for all NAFLD patients because of the risks of the procedure.

We have previously reported the usefulness of contrast enhancement ultrasound (CEUS) in the diagnosis of NASH with a contrast agent, Levovist, which is phagocytosed by the Kupffer cells (KC) in the liver.[8,9] In the liver parenchyma of NASH patients, the accumulation of Levovist microbubbles decreased remarkably 5 min after Levovist injection (especially by 20 min).

823